Static Vs. Dynamic Regenerator Assignment in Optical Switches: Models and Cost Trade-offs

Kotikalapudi Sriram, David Griffith, Richard Su, and Nada Golmie

***Abstract*— Agile all optical switches (OXC) currently use an architecture in which regenerators and transceivers have pre-assigned fixed directionality. However, technology is evolving to enable new OXC architectures in which the directionality of regenerators and transceivers can be dynamically assigned on demand. In this paper, we quantify the performance and cost benefits of regenerators and transceivers with dynamically assignable directionality. We show that fewer regenerators and transceivers need to be used with the new architecture because of sharing of resources across all directionality combinations. This translates to significant cost savings for the new architecture, especially as the traffic load in the network increases.**

***Index Terms*— regenerators, switch architecture, optical cross connects (OXCs), agile optical networks, performance metrics**

I. Introduction

It is generally well known that there are significant cost advantages with respect to both capital expenditures (capex) and operational expenditures (opex) associated with deploying OXC-based agile all optical networks instead of conventional optical networks using Optical-Electrical-Optical (OEO) switching [1]–[4]. Agile all optical networks save on regenerator costs by selective use of regenerators at transit nodes only when required to regenerate an optical signal for an individual wavelength connection [2],[5]. In contrast, the OEO switched network uses a regenerator for each wavelength at each transit node in the connection path. Additionally, further technology advancements allow agile optical networks to be even more economical in terms of regenerator and transceiver cost savings. This additional advantage is due to evolving technology which allows use of (1) dynamically assignable directionality for regenerators and (2) dynamically assignable I/O port associations for transceivers. This paper examines the benefits of an optical switch architecture that we propose based on this new technology.

The existing and proposed technologies for optical switches are respectively called the Static Assigned Regenerator and Transceiver (SART) and Dynamically Assignable Regenerator and Transceiver (DART) architectures, shown in Fig. 1 and Fig. 2. For an OXC switch of size $N \times N$, there are N ports and $N(N-1)/2$ input/output port-pairs. In the SART architecture, a dedicated pool of regenerators is used for each of the $N(N-1)/2$ port-pairs. Although not explicitly shown in Fig. 1, a dedicated transceiver (TR) pool is also used for each of the N fiber ports for add/drop of wavelengths. Splitters/combiners and Tunable I/O (TIO) devices are used at each fiber port to direct the appropriate wavelengths to the corresponding regenerator pools and TRs. The SART architecture is commonly used in the current implementations of agile all optical networks. The DART architecture, shown in Fig. 2, uses an additional switch stage, called OXC adjunct, to extract/inject the wavelengths that need regeneration or add/drop via TRs. Here the directionality of each regenerator and TR is dynamically assignable. Thus, in the DART architecture, it is possible to have one single shared pool of regenerators as well as one single shared pool of TRs. There is additional cost associated with this architecture due to the presence of the OXC adjunct as well as the more complex TIO devices. However, there is a possibility for that additional cost to be significantly offset due to savings in regenerator and TR costs, which are usually a significant fraction of the total switch cost. The sharing of regenerators and TRs in the DART architecture allows a desired connection blocking probability to be achieved at the switching node while using fewer regenerators and TRs than what is required by the SART architecture.

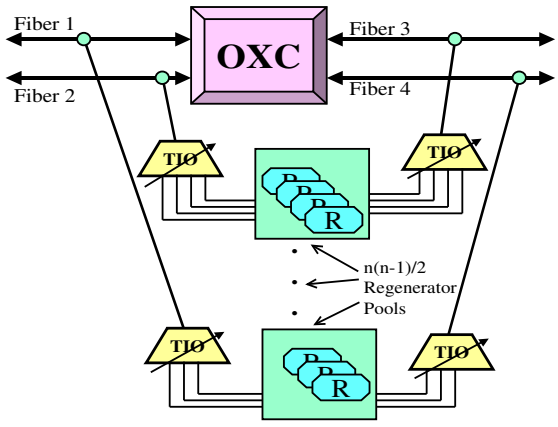

Fig. 1. Switch architecture associated with dynamically allocated regenerators and TR modules (SART architecture).

Our objective in this paper is to quantitatively compare the SART and DART architectures. In Section II, we present an analytical model based on the assumption of Poisson connection arrivals. In Section III, we describe our simulation model that can incorporate any connection interarrival and

K. Sriram, D. Griffith, and N. Golmie are with the National Institute of Standards and Technology (NIST), Gaithersburg, MD 20899 USA (contact e-mail: ksriram@nist.gov).

R. Su is with the Department of Electrical & Computer Engineering, University of Maryland, College Park, MD 20742 USA

This research was partially supported by the Laboratory for Telecommunications Sciences (LTS), the Defense Advanced Research Projects Agency (DARPA) Fault Tolerant Networks (FTN) program, and the National Communications System (NCS).

Report Documentation Page

Form Approved
OMB No. 0704-0188

1. REPORT DATE	2. REPORT TYPE	3. DATES COVERED
APR 2004		**00-00-2004 to 00-00-2004**

4. TITLE AND SUBTITLE	5a. CONTRACT NUMBER
Static Vs. Dynamic Regenerator Assignment in Optical Switches: Models and Cost Trade-offs	5b. GRANT NUMBER
	5c. PROGRAM ELEMENT NUMBER
6. AUTHOR(S)	5d. PROJECT NUMBER
	5e. TASK NUMBER
	5f. WORK UNIT NUMBER
7. PERFORMING ORGANIZATION NAME(S) AND ADDRESS(ES) **National Institute of Standards and Technology,Gaithersburg,MD,20899**	8. PERFORMING ORGANIZATION REPORT NUMBER
9. SPONSORING/MONITORING AGENCY NAME(S) AND ADDRESS(ES)	10. SPONSOR/MONITOR'S ACRONYM(S)
	11. SPONSOR/MONITOR'S REPORT NUMBER(S)

12. DISTRIBUTION/AVAILABILITY STATEMENT
Approved for public release; distribution unlimited

13. SUPPLEMENTARY NOTES
Proceedings of the IEEE Workshop on High Performance Switching and Routing (HPSR 2004), April 2004, Phoenix, AZ, pp. 151-155

14. ABSTRACT
see report

15. SUBJECT TERMS

16. SECURITY CLASSIFICATION OF:			17. LIMITATION OF ABSTRACT	18. NUMBER OF PAGES	19a. NAME OF RESPONSIBLE PERSON
a. REPORT **unclassified**	b. ABSTRACT **unclassified**	c. THIS PAGE **unclassified**	**Same as Report (SAR)**	**5**	

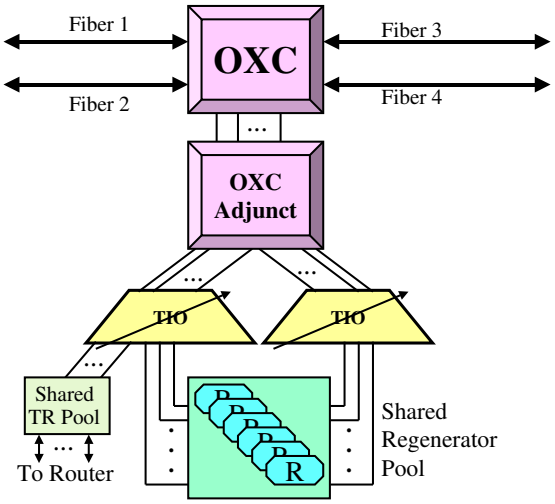

Fig. 2. Switch architecture associated with statically configured regenerators and TR modules (DART architecture).

holding time distributions. In Section IV, we present our numerical results and discuss their implications. We state our conclusions in Section V.

II. Analytical Model

In order to carry out an analysis of the relative cost of the two switch architectures, we first develop expressions for the blocking probability associated with deploying the SART and DART architectures. In both cases the OXC has N bidirectional fiber ports, each of which may support multiple wavelengths. The number of possible input/output port pairs is ${}_NC_2 = N(N-1)/2$. In the following analysis, we assume that the OXC has four fiber ports, as shown in Fig. 3, which gives us six possible (input port, output port) combinations.

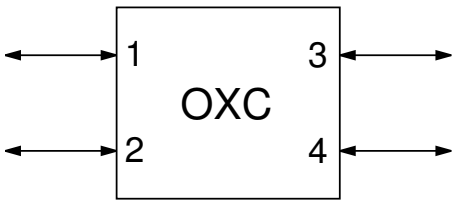

Fig. 3. OXC with four bidirectional fiber ports. The following ordered pairs denote the six possible paths through the switch: (1,2), (1,3), (1,4), (2,3), (2,4), and (3,4).

The cost of a transceiver (TR) is very close to that of a regenerator. This is because the optoelectronics and electronic circuitry used in them are almost the same. Hence, for simplicity of modeling we assume that any connection that requires a TR is equivalent to one that requires a regenerator. We therefore use a single parameter in our models for the fraction of connections that require a regenerator (or equivalently a TR).

The majority of the connection requests going through a switch do not require regenerators. They simply pass through the OXC. We assume that the net arrival rate directed to the regenerators is λ. In both the SART and DART theoretical models, connection request arrivals follow a Poisson process with rate λ; each regenerator is represented by a server whose rate μ is the inverse of the mean connection holding time.

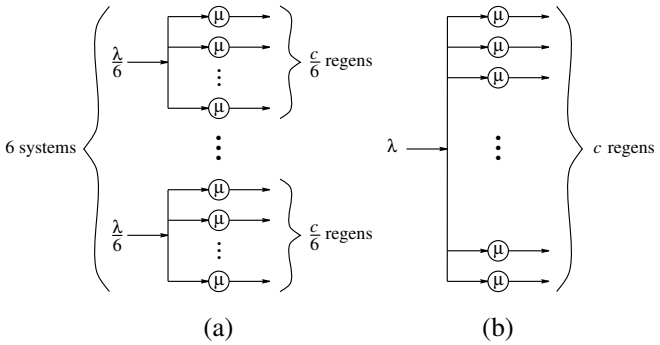

Fig. 4. (a): Queueing model for the SART switch using 6 sets of c' regenerators, where the probability that an arrival will be directed to a given set of servers is uniform. (b): Queueing model for the DART switch using c regenerators with single arrival source.

In the SART architecture, shown in Fig. 1, we assume that an equal number of regenerators are assigned to each of the ${}_NC_2$ input/output port pairs. If the total number of regenerators in the switch is c, then $c' = 2c/(N^2 - N)$ regenerators are available to each port pair. This situation is shown in Fig. 4(a). In this case, we have $(N^2-N)/2$ $M/G/c'/c'$ systems, each of which receives connection requests at a rate of $\lambda' = 2\lambda/(N^2-N)$. The blocking probability for connections requiring the use of any given input/output port pair is $B(c', \rho')$, where $\rho' = \lambda'/\mu$ is the directional regenerator load, measured in Erlangs, and

$$B(c', \rho') = \frac{(\rho')^{c'}/c'!}{\sum_{k=0}^{c'}(\rho')^k/k!} \tag{1}$$

is the well-known Erlang-B loss formula. In the DART architecture, the OXC uses a set of c dynamically allocated regenerators, as shown in Fig. 2. We can use a $M/G/c/c$ queueing model, shown in Fig. 4(b), in this case. The blocking probability associated with this model is $B(c, \rho)$, where $\rho = \lambda/\mu$ is the total switch regenerator load, measured in Erlangs.

Given a particular switch architecture and a known load level, we can use the inverse of the Erlang-B loss formula to determine the minimum number of regenerators that are required to achieve a blocking probability that is below a given threshold, $P_{\max}$. Once we obtain this quantity, $c_{\min} = B^{-1}(P_{\max}, \rho)$, we can determine the associated cost of the switch that satisfies the blocking probability requirement at the indicated load. For the cost comparison that we describe in Section IV, we assume that the cost of an adjunct OXC is roughly equivalent to the cost of the primary OXC. We also assume that the cost of a regenerator is the same in each of the two architectures, and is given by $f \cdot O$, where O is the cost of a primary or adjunct OXC and f is the fraction of the OXC's cost associated with a single regenerator. Thus, the cost of switches using the DART and SART architectures that achieve a maximum blocking probability of $P_{\max}$ at a load of

ρ is given as a multiple of OXC cost by

$$C_{\mathrm{DART}} = 2 + f \cdot B^{-1}(P_{\max}, \rho) \quad (2)$$
$$C_{\mathrm{SART}} = 1 + f \cdot B^{-1}(P_{\max}, \rho'). \quad (3)$$

III. Simulation Model

We use a simulation model, implemented in C++, that incorporates discrete event processing. The connection holding time distribution is shown in Fig. 5. This distribution is motivated by the observation that in the near future wavelength connections can be expected to be requested for durations on the order of a fraction of a day. The average connection duration is 3.55 hours for the distribution in Fig. 5. The connection arrival process is assumed to be either a Poisson process (smooth arrivals) or a bursty process represented by hyper-exponential interarrival times. The hyper-exponential density function for two arrival modes is given by

$$f_X(x) = p\lambda_1 \exp(-\lambda_1 x) + (1-p)\lambda_2 \exp(-\lambda_2 x), \quad (4)$$

where we assume without loss of generality that $\lambda_1 > \lambda_2$, and where p is the probability of being in mode 1 where arrivals occur at the higher rate of λ_1, and $(1-p)$ is the probability of being in mode 2 where arrivals occur at the lower rate λ_2. The ratio of arrival rates, θ, and the average arrival rate, λ, are

$$\theta = \lambda_1/\lambda_2 \quad (5)$$

and

$$\lambda = \left(p\lambda_1^{-1} + (1-p)\lambda_2^{-1}\right)^{-1}, \quad (6)$$

and the co-efficient of variation of the arrival process is given as follows:

$$\chi^2 = \frac{\mathsf{Var}\{X\}}{(\mathsf{E}\{X\})^2} = \frac{2(p + (1-p)\theta^2)}{(p + (1-p)\theta)^2} - 1. \quad (7)$$

We chose the parameters of the hyper-exponential distribution to obtain different values of the net packet arrival rate λ (equivalently, Erlang load) and χ^2 in the simulations. For example, the values of p = 0.95, θ = 40 give χ^2 = 17.6, and p = 0.9, θ = 10 give χ^2 = 5.04. This allows different burstiness measures to be incorporated in the simulation runs.

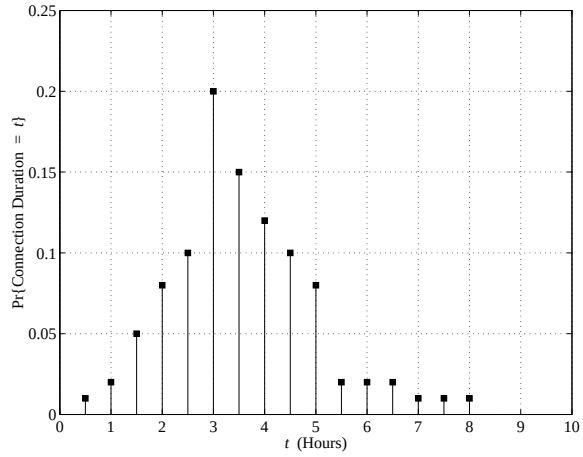

Fig. 5. Probability mass function for the duration of connections used in the simulations

In the simulation of the SART switch architecture, there are six directional-pairs involved for a switch size of $N = 4$. We direct connection arrivals with equal probability to each directional-pair, simulate each directional-pair independently, and then take the worst of the six performance metrics to obtain the blocking probability for the switch.

IV. Numerical Results and Discussion

We first validate our simulation methodology by comparing the results of the $M/G/c/c$ analysis in Section II with those obtained from simulations. Table I and Table II show these comparisons for connection blocking probability due to regenerator unavailability for the DART and SART architectures, respectively. The extremely close comparison in numbers in these two tables is a very good validation of our simulation modeling tool. In both cases our error was on the order of 0.1% except for the DART architecture at loads of 10–25 Erlangs, where the error was on the order of 1%. We proceed to present a variety of steady-state and transient results based on simulations, including the effects of burstiness in the arrival process.

TABLE I

Theoretical and experimental values of blocking probability for dynamic regenerator and TR module placement.

Load (Erlangs)	$B(c, \rho)$	Experiment
10	7.3176E-05	7.4444E-05
15	8.3935E-03	8.2933E-03
20	6.6097E-02	6.6470E-02
25	1.6798E-01	1.6685E-01
30	2.7090E-01	2.7032E-01
35	3.5845E-01	3.5775E-01
40	4.2995E-01	4.3000E-01
45	4.8827E-01	4.8811E-01
50	5.3630E-01	5.3623E-01

TABLE II

Theoretical and experimental values of blocking probability for static regenerator and TR module placement.

Load (Erlangs)	$B(c', \rho')$	Experiment
10	6.2444E-02	6.2478E-02
15	1.4992E-01	1.4953E-01
20	2.4258E-01	2.4236E-01
25	3.2652E-01	3.2569E-01
30	3.9834E-01	3.9794E-01
35	4.5871E-01	4.5730E-01
40	5.0939E-01	5.0878E-01
45	5.5214E-01	5.5277E-01
50	5.8850E-01	5.8875E-01

Fig. 6 shows transient behavior taken from a single simulation run and compares the numbers of regenerators used in the SART and DART switch architectures over a 24-hour period. It is evident from the plots that the DART switch makes better use of the available regenerators, and implicitly blocks fewer connection requests. Even though the regenerator utilization of the SART switch is lower than that of the DART switch in this example, the SART blocking probability is higher because regenerators cannot be made available where they are needed. Thus resources for one direction can sit idle while connection

requests are blocked at another input/output port pair for lack of resources.

Fig. 7 plots the connection request blocking probability, P_B, for the SART and DART switches for 18 and 24 regenerators. In the SART architecture, the available regenerators are distributed equally across the 6 directional regenerator pools (see SART switch architecture in Fig. 1). The advantage of a shared regenerator pool in the DART switch in terms of lower blocking probability is evident from these plots. Also evident is the fact that adding more regenerators reduces the blocking probability significantly, with greater reductions in the case of the DART switch.

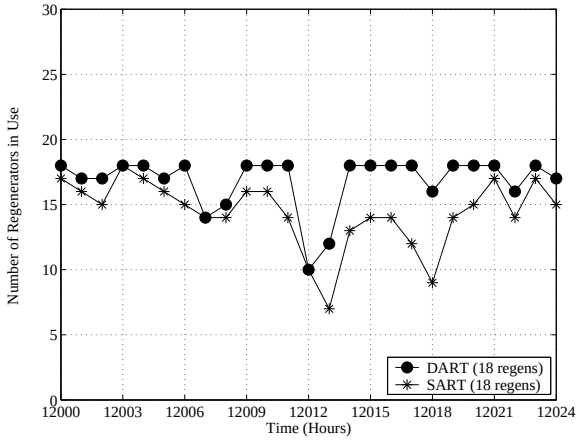

Fig. 6. Performance histories for DART and SART switch architectures using 18 regenerators under a load of 30 Erlangs.

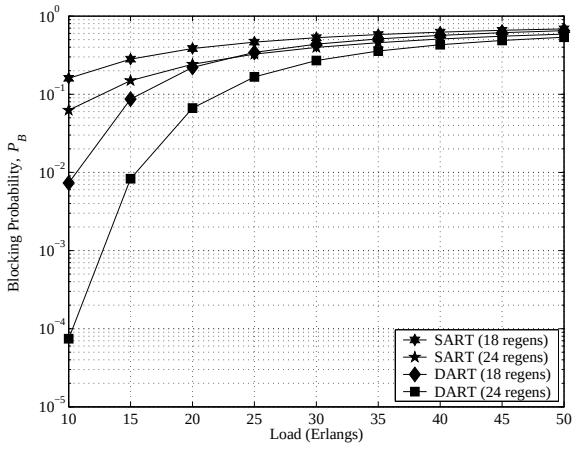

Fig. 7. New connection blocking probability for DART and SART switch architectures using 18 and 24 regenerators under a range of loads.

Fig. 8 shows the number of regenerators required to achieve a connection blocking probability of at most $P_{\max} = 10^{-3}$ over a range of traffic loads. The figure shows a comparison of the theoretical and simulation results for the $M/G/c/c$ case. In the plots, the analytical results are indicated by solid and dashed lines and the simulation results are denoted by markers. For the SART switch, the $M/G/c/c$ analysis produces a staircase function with a step size of six because the regenerators are determined for any one direction and multiplied by six to give the number for the whole switch. We note that for both the SART and DART switch architectures, the difference between the number of required regenerators obtained from the theoretical analysis and the simulation results is very small. A service provider can use results such as those in Fig. 8 to determine the number of regenerators (and TRs) needed by an OXC switch to achieve a desired blocking probability for a given load level.

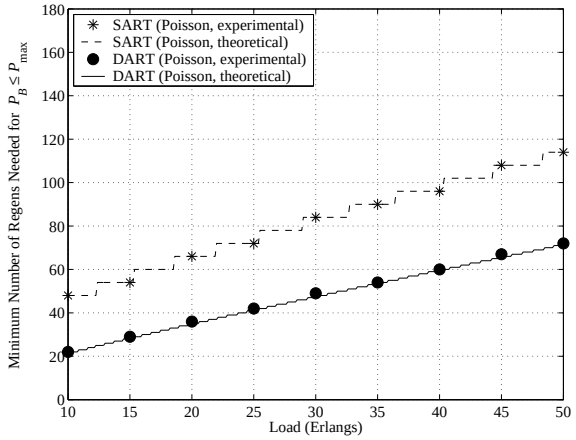

Fig. 8. Comparison of experimental results with theoretical predictions for the number of regenerators required to achieve a new connection blocking probability of at most 0.001. Connection arrivals follow a Poisson process.

Fig. 9 shows a comparison of the numbers of regenerators required to achieve $P_B \leq 0.001$ in the cases of a Poisson (smooth, χ^2 = 1) arrival process and a bursty ($\chi^2 = 18$) arrival process with hyper-exponential interarrival times. It is evident that DART uses significantly fewer regenerators as compared to SART, in both the Poisson and hyper-exponential cases.

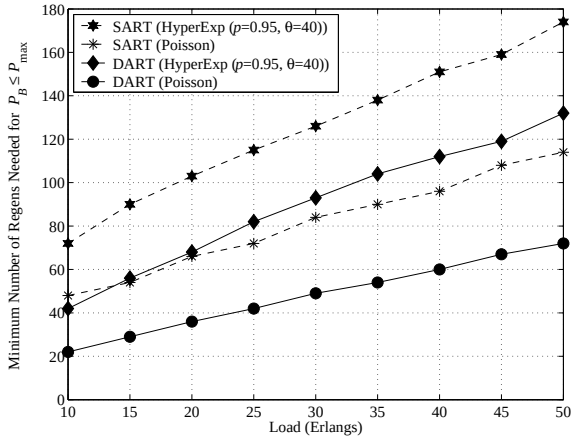

Fig. 9. Number of regenerators required to achieve a new connection blocking probability of 0.001 using DART and SART architectures with Poisson and hyper-exponential connection arrival processes.

Fig. 10 shows the number of regenerators required in the cases of hyper-exponential interarrival times with low burstiness and high burstiness. As the burstiness measure increases from $\chi^2 = 5$ to $\chi^2 = 18$, the required number of regenerators increases by more than 20% in both cases (SART or DART). More economic usage of regenerators in the case of DART

enables greater design robustness when fluctuations in traffic burstiness occur.

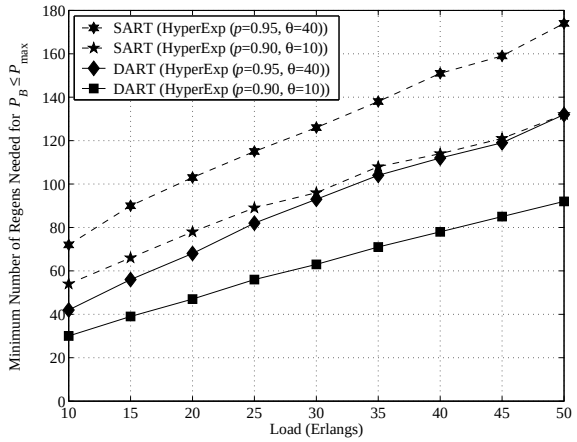

Fig. 10. Number of regenerators required to achieve a new connection blocking probability of 0.001 using DART and SART architectures with hyper-exponential connection arrival processes with different levels of burstiness.

Finally, Fig. 11 and Fig. 12 show comparisons of the costs of implementation of the SART and DART switch architectures over a range of traffic load values for fractional regenerator cost values of $f = 0.03$ and $f = 0.04$, respectively. The cost of a regenerator is known to be about 1/25th to 1/30th that of the OXC cost [5]. The initial cost of the DART implementation (excluding regenerators) is assumed higher by a factor of two as compared to the SART implementation (excluding regenerators). This is because of the added cost of the OXC adjunct and the need for potentially more complex TIOs (see SART and DART architectures in Fig. 1 and Fig. 2). As the traffic load increases, the SART architecture requires many more regenerators than the DART architecture. Hence, there is a critical load value, above which the DART architecture cost is lower than that of the SART architecture. The critical load value is much lower in Fig. 12 (about 12 Erlangs for both architectures) than in Fig. 11 (about 27 Erlangs for both architectures), where the regenerator cost is a higher fraction of the OXC cost. Fig. 11 and Fig. 12 also demonstrate that the critical load value (at which DART becomes less costly than SART) is not very sensitive to the traffic burstiness but is quite sensitive to the regenerator cost factor f. This critical point can shift significantly to an even lower load value if we consider the opex for power consumption and footprint, because regenerators consume power as well as shelf space. The use of fewer regenerators for the DART architecture would also result in lower opex costs as compared to those associated with the SART architecture.

V. Conclusions

In this paper, we compared two alternative all-optical switch architectures that differ in the way the regenerators and TRs are used: static assigned (SART) vs. dynamically assigned (DART). We showed that there are significant quantitative performance and cost benefits due to the shared resource arrangement in the DART architecture. These benefits will be even further enhanced when the power consumption and

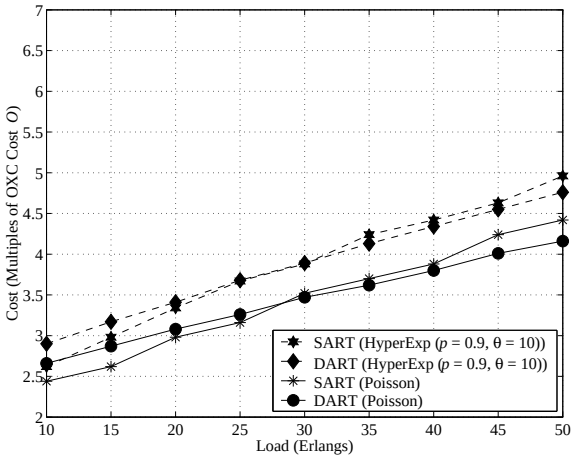

Fig. 11. Cost of DART and SART architectures as a multiple of OXC cost O when $f = 0.03$, for hyper-exponential and Poisson arrival processes.

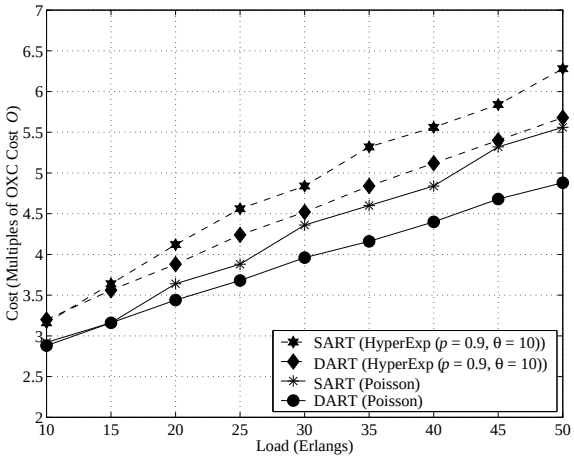

Fig. 12. Cost of DART and SART architectures as a multiple of OXC cost O when $f = 0.04$, for hyper-exponential and Poisson arrival processes.

form factor considerations are incorporated into the cost models. As part of our ongoing work, we are performing further simulations of the problem studied here in a larger network simulation environment where we model the effect of wavelength reach; this work is being done using NIST's GLASS simulation tool [6].

References

[1] ITU-T Recommendation G.8080/Y.1304, "Architecture of the automatically switched optical network (ASON)" (International Telecommunication Union-Telecommunication Standardization Sector, November 2001), http://www.itu.int/ITU-T/

[2] B. Doshi, et al, "Transparent Cross-Connect and Ultra-Long-Reach Transmission Systems: Complementary Technologies", NFOEC 2001 Technical Proceedings.

[3] G.P. Agrawal, "Fiber-Optic Communication Systems," 1997.

[4] R. Ramaswami and K. N. Sivarajan, Optical Networks - A Practical Perspective, 2002.

[5] A. Solheim, "Agile Photonic Networking," World Markets Series: Global Optical Communications World Markets Whitepaper, July 2002.

[6] Oliver Borchert, Richard Rouil, "The GMPLS Lightwave Agile Switching Simulator - An overview," www.antd.nist.gov/glass